

## Supplementary Information

### Gold Nanoclusters with Bright Near-Infrared Photoluminescence

*Goutam Pramanik, Jana Humpolickova, Jan Valenta, Paromita Kundu, Sara Bals, Petr Bour, Martin Dracinsky, and Petr Cigler\**

#### Materials

All reagents were purchased from commercial sources and used as received. Aqueous solutions in all experiments were prepared using Milli-Q water. 3-(aminopropyl)triphenylphosphonium (TPP) bromide salt was prepared as described in the literature.<sup>1</sup> The corresponding chloride, iodide, and tetrafluoroborate salts of TPP were obtained by exchange of the Br<sup>−</sup> salt on an anion exchange column loaded with Amberlite<sup>®</sup> IRA-400 in the corresponding anion cycle, following published procedures.<sup>2</sup>

#### Determination of Quantum Yield

Quantum yield (QY) were measured by a relative comparison method using the following equation

$$QY_{sample} = QY_{ref} * \frac{F_{sample}}{F_{ref}} * \frac{A_{ref}}{A_{sample}} * \frac{\eta_{sample}^2}{\eta_{ref}^2}$$

(Equation

S1)

where F, A, and  $\eta$  are the measured fluorescence intensity (integrated areas of photoluminescence spectra of the AuNCs and Rhodamine 6G in the region between 500 – 850 nm), the absorbance at the excitation wavelength (480 nm), and the refractive index of the solvent, respectively. The subscripts “sample” and “ref” stand for AuNC samples and reference (Rhodamine 6G) respectively. The emission spectra of the **1** and **2** were measured in water and Rhodamine 6G was measured in ethanol upon excitation at 480 nm at the same conditions. Following this, the areas under the curves were determined using Microsoft Excel. To avoid inner filter effects, the absorption of the AuNCs and reference were kept below 0.05 at the excitation wavelength (480 nm). The refractive index for water is 1.33 ( $\eta_{sample}$ ), and for ethanol is 1.36 ( $\eta_{ref}$ ). All the measurements were performed at 25 °C. QY<sub>ref</sub> is the quantum yield of the Rhodamine 6G (0.95) in ethanol at 25 °C.

**Table S1.** Calculation of quantum yields of the AuNCs.

Samples	$A_{sample}$ (at 480 nm)	$A_{ref}$ (at 480 nm)	$F_{sample}$	$F_{ref}$	$\eta_{sample}$	$\eta_{ref}$	QY <sub>ref</sub>	QY <sub>sample</sub>
<b>1</b>	0.0395	0.0322	1836	12915	1.33	1.36	0.95	0.1053
<b>2</b>	0.0396	0.0322	4505	12915	1.33	1.36	0.95	0.2576

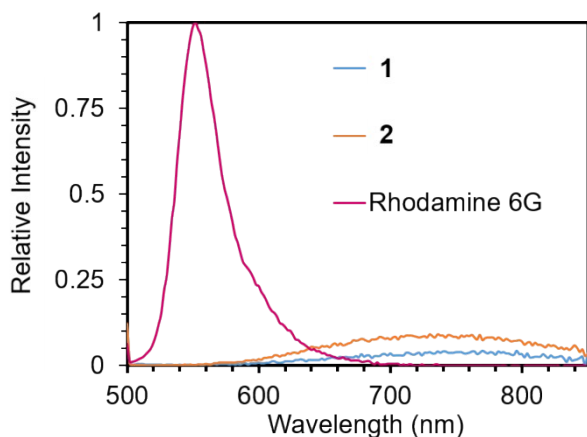


**Fig. S1** Normalized emission spectra of aqueous solutions of **1**, **2** ( $X^- = \text{BF}_4^-$ ) and Rhodamine 6G collected upon excitation at 480 nm.

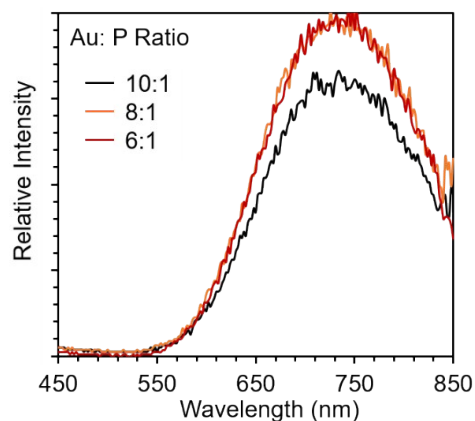


**Fig. S2** Relative emission spectra of aqueous solutions of **2** at different Au:P ratio upon excitation at 365 nm.

### X-ray photoelectron spectroscopy (XPS) measurements

XPS measurements were performed using Omicron Nanotechnology equipment. The primary X-ray beam was monochrome radiation from an Al lamp with an energy of 1486.7 eV. The constant analyzer energy (CAE) mode was used, and intensity calibration was based on copper and copper spectra-derived calibration constants. The ion gun used argon ions with an energy of  $\sim 5$  keV; ion etching was carried out in the preparation chamber. A circular area with a diameter of approximately 0.8 mm was used for analysis. Measured spectra were evaluated with CasaXPS software. The binding energy of a known element (usually C 1s with binding energy 284.8 eV) was used for calibration of the binding energy axis.

### Photoluminescence lifetime measurements

The photoluminescence lifetime measurements were carried out using a time correlation single photon counting (TCSPC) system integrated into Fluoromax-4 (Horiba). We used a pulsed excitation signal at 370 nm with a repetition rate of 1 MHz, provided by a NanoLED-370 light source (100 ps, fwhm), and the emission was collected using a TBX photomultiplier detector. We note the temperature-dependent study concentrates only on the slow component of luminescence decay. We fitted the photoluminescence decay by three exponentials using equation (1), but it can be fitted also by a distribution of lifetimes, for example by a stretched exponential (Kohlrausch) function

$$I(t) = Ae^{\left(-\frac{t}{\tau}\right)^\beta}, \quad (\text{Equation S2})$$

where parameter  $\beta$  is around 0.6. This value indicates that we have a process with certain distribution of lifetimes, e. g. due to variation of ligands and their conformations. For evaluation of the temperature evolution of emission rate we use just the most representative lifetime, i. e. an average lifetime (obtained by the integration method, i. e. independent of the fitting model). The slow microsecond components of decay according to equation (1) look like minor compared to the nanosecond one, but this is due to the short pulse excitation which is not exciting slow processes efficiently.<sup>3</sup> We have checked that under long microsecond pulses the slow decay components largely dominates (nanosecond component is negligible or null; data not shown).

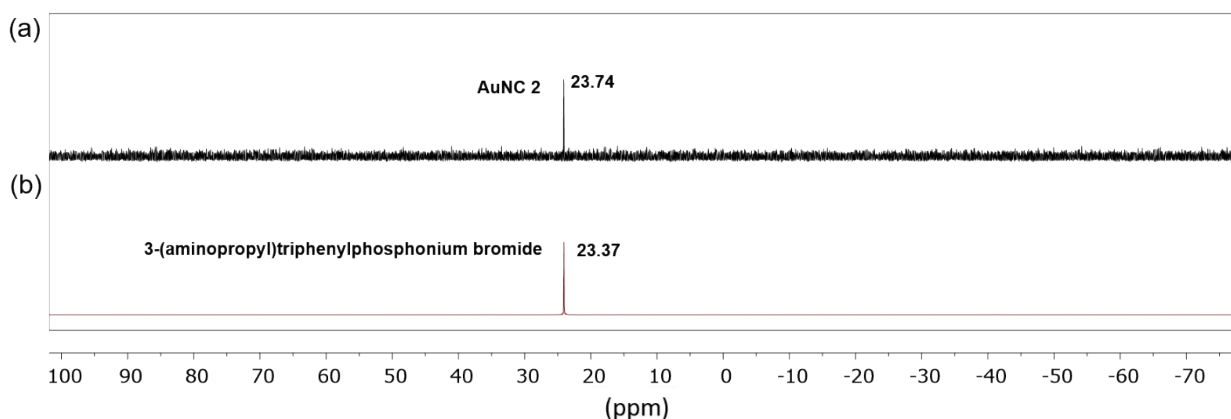
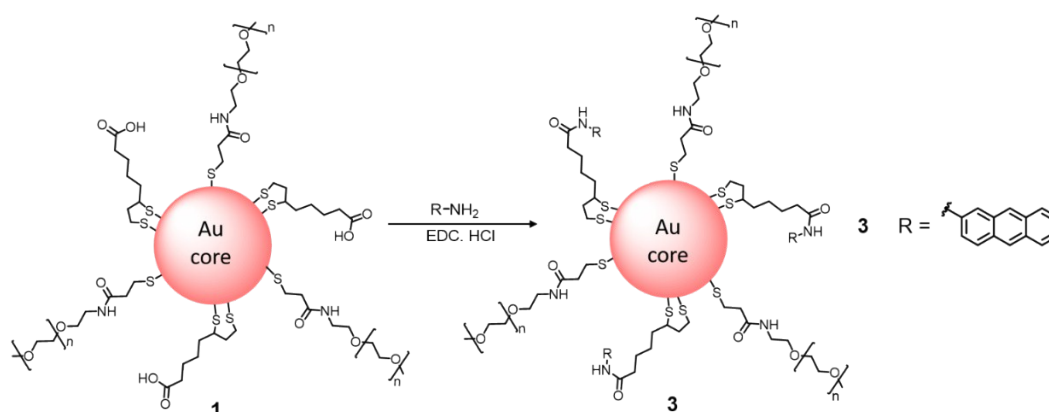
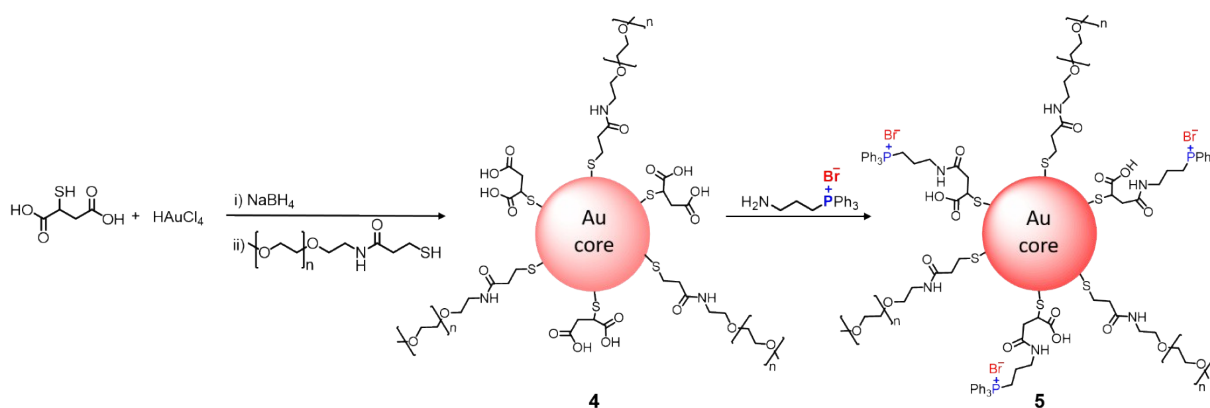


**Fig. S3**  $^{31}\text{P}$  NMR (161.98 MHz,  $\text{D}_2\text{O}$ ) of (a) **2** and (b) 3-(aminopropyl) triphenylphosphonium bromide. The peaks were assigned relative to  $\text{H}_3\text{PO}_4$  (0.00 ppm).



**Scheme S1.** Schematic representation of the structure and preparation of AuNC **3**.



**Scheme S2.** Schematic representation of the structure and preparation of mercaptosuccinic acid stabilized AuNCs **4** and **5**.

### Preparation of AuNC **3**

AuNC **1** solution (4 mL, 0.2 mg/mL) and excess of 2-aminoanthracene (6 mg, 31  $\mu\text{mol}$ ) solution in 1 mL DMSO were mixed together. Then the pH of the solution was adjusted to the range of 4.5–6.0 with 1 M HCl. The reaction was started by adding excess N-(3-

dimethylaminopropyl)-N'-ethylcarbodiimide hydrochloride (EDC.HCl) (10 mg, 52  $\mu$ mol) and stirred overnight. Then the reaction mixture was lyophilized. Then 4 mL water was added to the reaction mixture and sonicated for 2 minutes. Then the insoluble part was removed by filtration. The filtrate was purified by applying three cycles of centrifugation/filtration using a membrane filtration device (Millipore) with a molecular weight cut-off of 3 kDa to obtain AuNC **3** and the absorption and emission spectra were acquired immediately.

#### Preparation of AuNCs **4** and **5**

AuNC **4** was prepared using the same procedure as **1**, only mercaptosuccinic acid (2 mg, 13.3  $\mu$ mol) was used instead of TA. AuNC **5** was prepared from **4** by the same procedure as **2** from **1**.

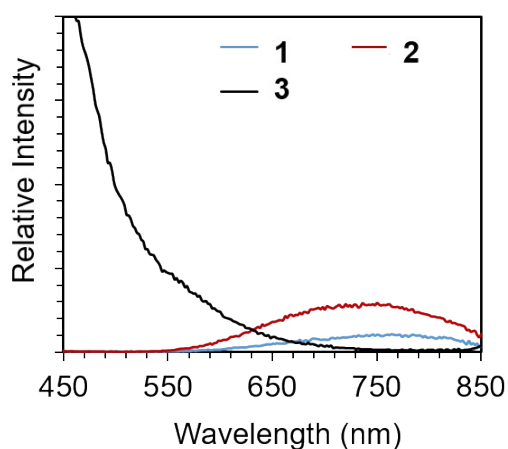


**Fig. S4** Relative photoluminescence spectra of aqueous solutions of AuNC **1**, **2** and **3** upon excitation at 365 nm.

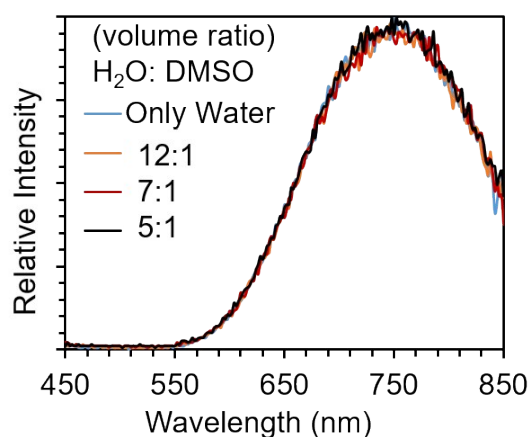


**Fig. S5** Relative photoluminescence spectra of aqueous and DMSO mixed solution of AuNC **2** upon excitation at 365 nm.

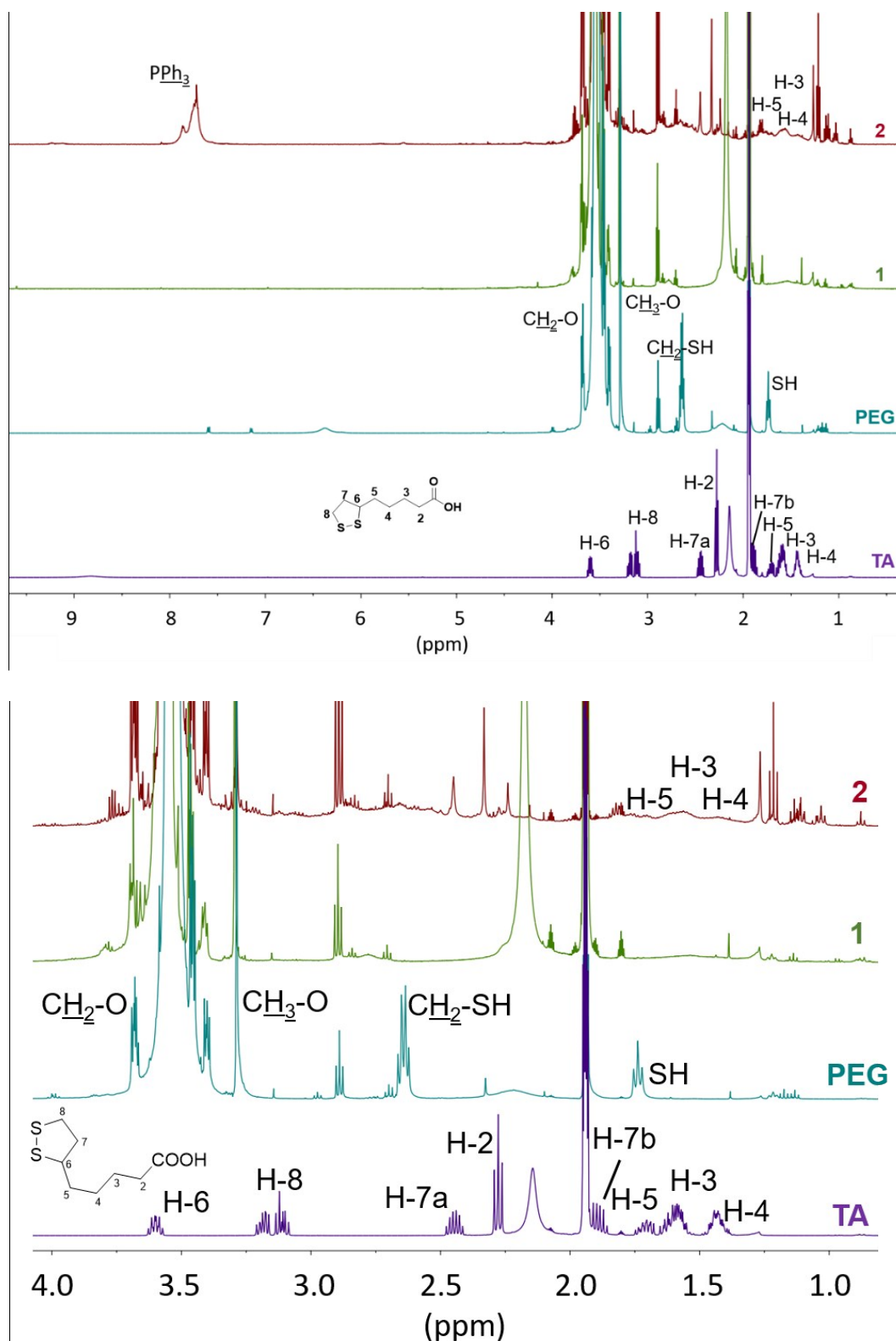


**Fig. S6** <sup>1</sup>H NMR (500 MHz, CD<sub>3</sub>CN) spectra of TA, thiol-terminated PEG, AuNC **1** and **2**. In the top panel the whole spectra are shown, the bottom panel shows detailed signal assignment. For estimation of ligand (PEG:TA) ratios on **2**, the following peaks were integrated: terminal CH<sub>3</sub>-O group on PEG (3H, 3.20 ppm) and sum of selected methylene groups from TA (6H, 1.24 – 1.80 ppm). For estimation of TPP:TA ratio, the aromatic region of TPP (15H, 7.43 – 7.95 ppm) was used and the same methylene groups for TA as above.

## Computations

To understand the AuNCs fluorescence properties, we constructed a simpler molecular model, where centered icosahedral  $\text{Au}_{13}$  core is connected to one TPP molecule (Fig. S7). The initial  $\text{Au}_{13}$  geometry was taken from the X-ray structure of a larger 25-atom cluster,<sup>4</sup> initial TPP and  $\text{Au}_{13}\text{TPP}$  geometries were constructed with a fully extended TPP backbone.  $\text{Au}_{13}$  was negatively and TPP,  $\text{Au}_{13}\text{TPP}$  were positively charged. Then geometries of the systems were optimized by energy minimization at the BP86/<sup>5</sup>6-31G\*\* level; the MWB60<sup>6</sup> pseudopotential and basis set was used to Au atoms and the Grimme's GD2 dispersion correction<sup>7</sup> applied. The Gaussian program<sup>8</sup> was used for all the quantum-chemical computations. For the optimized structures energies of the excited states were calculated using the time dependent density functional theory.<sup>9</sup> Qualitatively similar results were obtained using the B3LYP<sup>10</sup> functional and CPCM<sup>11</sup> model for a solvent environment.

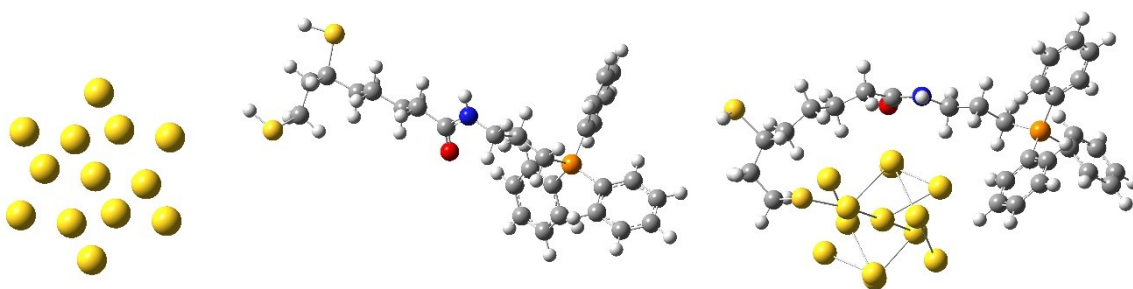


**Fig. S7** Optimized geometries of the  $\text{Au}_{13}^-$ ,  $\text{TPP}^+$  and  $\text{Au}_{13}\text{TPP}^+$ . The following color code is used: Au – yellow (larger spheres), S – yellow, C – grey, H – white, O – red, N – blue, P – orange.

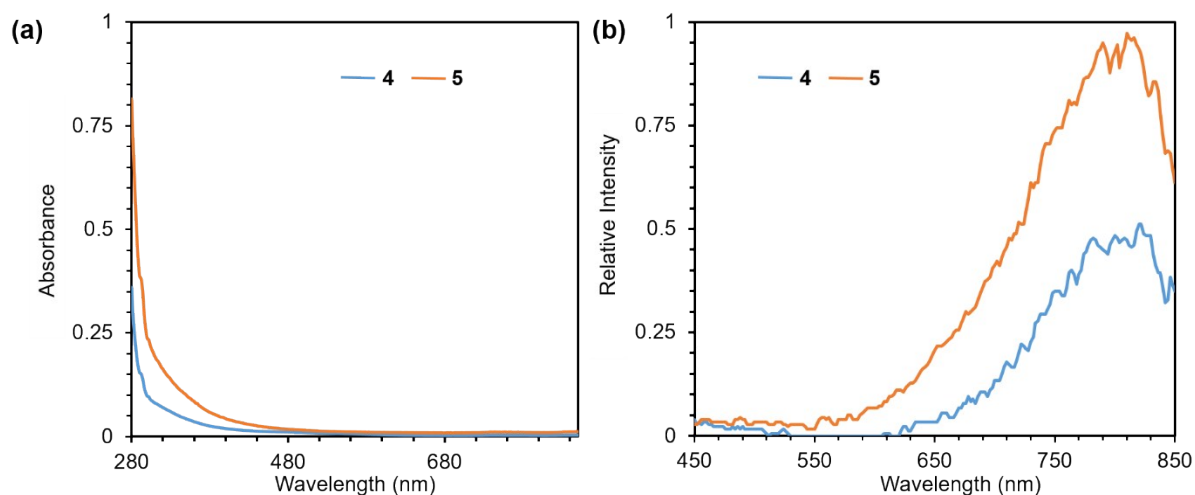


**Fig. S8** (a) Normalized absorption spectra of aqueous solutions of AuNC **4** and **5**. (b) Normalized emission spectra of aqueous solutions of **4** and **5** collected upon excitation at 365 nm.

## References

- 1 C.-J. Zhang, J. Wang, J. Zhang, Y. M. Lee, G. Feng, T. K. Lim, H.-M. Shen, Q. Lin and B. Liu, *Angew. Chem.*, 2016, **128**, 13974–13978.
- 2 V. J. A. Jameson, H. M. Cochemé, A. Logan, L. R. Hanton, R. A. J. Smith and M. P. Murphy, *Tetrahedron*, 2015, **71**, 8444–8453.

- 3 M. Greben and J. Valenta, *Rev. Sci. Instrum.*, 2016, **87**, 126101.
- 4 M. Zhu, C. M. Aikens, F. J. Hollander, G. C. Schatz and R. Jin, *J. Am. Chem. Soc.*, 2008, **130**, 5883–5885.
- 5 J. P. Perdew, *Phys. Rev. B*, 1986, **33**, 8822–8824.
- 6 D. Figgen, G. Rauhut, M. Dolg and H. Stoll, *Chem. Phys.*, 2005, **311**, 227–244.
- 7 S. Grimme, *J. Comput. Chem.*, 2006, **27**, 1787–1799.
- 8 M. J. Frisch, G. W. Trucks, H. B. Schlegel, G. E. Scuseria, M. A. Robb, J. R. Cheeseman, G. Scalmani, V. Barone, G. A. Petersson, H. Nakatsuji, X. Li, M. Caricato, A. V. Marenich, J. Bloino, B. G. Janesko, R. Gomperts, B. Mennucci, H. P. Hratchian, J. V. Ortiz, A. F. Izmaylov, J. L. Sonnenberg, Williams, F. Ding, F. Lipparini, F. Egidi, J. Goings, B. Peng, A. Petrone, T. Henderson, D. Ranasinghe, V. G. Zakrzewski, J. Gao, N. Rega, G. Zheng, W. Liang, M. Hada, M. Ehara, K. Toyota, R. Fukuda, J. Hasegawa, M. Ishida, T. Nakajima, Y. Honda, O. Kitao, H. Nakai, T. Vreven, K. Throssell, J. A. Montgomery Jr., J. E. Peralta, F. Ogliaro, M. J. Bearpark, J. J. Heyd, E. N. Brothers, K. N. Kudin, V. N. Staroverov, T. A. Keith, R. Kobayashi, J. Normand, K. Raghavachari, A. P. Rendell, J. C. Burant, S. S. Iyengar, J. Tomasi, M. Cossi, J. M. Millam, M. Klene, C. Adamo, R. Cammi, J. W. Ochterski, R. L. Martin, K. Morokuma, O. Farkas, J. B. Foresman and D. J. Fox, *Gaussian 16*, Wallingford, CT, 2016.
- 9 F. Furche and R. Ahlrichs, *J. Chem. Phys.*, 2002, **117**, 7433–7447.
- 10 A. D. Becke, *J. Chem. Phys.*, 1993, **98**, 5648–5652.
- 11 A. Klamt and G. Schüürmann, *J. Chem. Soc. Perkin Trans. 2*, 1993, **0**, 799–805.